Supplement of Atmos. Chem. Phys., 22, 15637–15657, 2022
https://doi.org/10.5194/acp-22-15637-2022-supplement

Atmospheric Chemistry and Physics
Open Access
EGU

Supplement of

Photolytic modification of seasonal nitrate isotope cycles in East Antarctica

Pete D. Akers et al.

Correspondence to: Pete D. Akers (pete.akers@tcd.ie)

Supplementary information for Photolytic modification of seasonal nitrate isotope cycles in East Antarctica

Supplementary Text S1. MARv3.12.1 details

Monthly surface mass balance data are provided by Modèle Atmosphérique Régional (MAR) v3.12.1 run at a 35 km resolution over Antarctica and driven at its lateral boundaries by 6 hr ERA5 data for the period 1979–2021 (Agosta et al., 2019; Amory et al., 2021). The results from MARv3.12.1 has not yet been published, but it has a similar performance to the well-documented MARv3.11 (Amory et al., 2021, Amory pers. comm., 2022). We determined uncertainties for the MARv3.12.1 SMB output on a drainage basin-specific basis by comparing in situ SMB observations with modeled SMB estimates. Root mean square errors (RMSE) for inclusive SMB intervals of [0, 50, 100, 300, 1500] kg m^{-2} a^{-1} were computed by comparing in situ SMB observations to MAR output SMB. In situ observations were taken from the SAMBA dataset (Favier et al., 2013) and updated with observations from Wang et al. (2016) and yearly values of shallow ice cores as used in Antarctic SMBMIP (Mottram et al., 2021; Thomas et al., 2017).

Modeled SMB values used in the uncertainty estimation were interpolated to the in situ observation locations using a four-nearest-neighbors inverse-distance-weighted method. Next, all the interpolated SMB values contained in the same grid cell were averaged as well as the observations to create 780 initial grid cell comparison pairs to calculate RSME values. We used only 80% (i.e., 624) of the observation pairs that best matched with MAR estimates in order to remove the largest outliers that might also involve measurement errors that cannot be well-quantified. A curve was then constructed of RSME vs. SMB bin and approximated with a simple linear fit to produce an error function in SMB in kg m^{-2} a^{-1}.

For each basin, we randomly generated 100000 errors (based on the previous error function) following a Monte-Carlo method applied to each model grid cell before integrating the SMB value at the scale of the whole basin. The SMB uncertainties are then estimated as the standard deviation of these 100000 basin-integrated SMB values.

Supplementary Table S1. Comparison of linear relationships between NO_3^- variables and pit depth at five sites. Coefficients and statistics are shown for the linear regressions of NO_3^- variables versus depth of sample in a snow pit. Coefficient values are given with ±1 standard error. Regressions with statistically significant ($p < 0.05$) *f-statistic* values are bolded.

Variable	*Slope*	*Intercept*	*F-statistic p-value*	r^2
	(ng g^{-1} · kg m^{-2} a^{-1} or kg m^{-2} a^{-1})	*(ng g^{-1} or unitless)*		
P1				
$\omega(NO_3^-)$	−0.47 ± 0.30	100 ± 17	0.13	0.07
$\delta^{15}N_{NO3}$	0.7 ± 1.2×10^{-4}	0.01 ± 0.01	0.56	0.01
$\delta^{18}O_{NO3}$	3.0 ± 4.4×10^{-5}	0.07 ± 0.00	0.51	0.01
$\Delta^{17}O_{NO3}$	−0.4 ± 1.5×10^{-5}	0.03 ± 0.00	0.80	0.00
P2				
$\omega(NO_3^-)$	−0.16 ± 0.19	76 ± 11	0.43	0.02
$\delta^{15}N_{NO3}$	−0.4 ± 1.1×10^{-4}	0.05 ± 0.01	0.76	0.00
$\delta^{18}O_{NO3}$	**2.2 ± 0.4×10^{-4}**	**0.09 ± 0.00**	**<0.01**	**0.46**
$\Delta^{17}O_{NO3}$	**−1.0 ± 0.2×10^{-4}**	**0.04 ± 0.00**	**<0.01**	**0.54**
P3				
$\omega(NO_3^-)$	**−0.75 ± 0.18**	**110 ± 10**	**<0.01**	**0.34**
$\delta^{15}N_{NO3}$	−7.5 ± 7.0×10^{-5}	0.03 ± 0.00	0.29	0.03
$\delta^{18}O_{NO3}$	**2.3 ± 0.5×10^{-4}**	**0.08 ± 0.00**	**<0.01**	**0.46**
$\Delta^{17}O_{NO3}$	**1.1 ± 0.1×10^{-4}**	**0.04 ± 0.00**	**<0.01**	**0.67**
P4				
$\omega(NO_3^-)$	**−0.95 ± 0.19**	**130 ± 11**	**<0.01**	**0.42**
$\delta^{15}N_{NO3}$	1.9 ± 1.0×10^{-4}	0.02 ± 0.01	0.08	0.09
$\delta^{18}O_{NO3}$	**−3.6 ± 0.3×10^{-4}**	**0.08 ± 0.00**	**<0.01**	**0.80**
$\Delta^{17}O_{NO3}$	**−1.2 ± 0.1×10^{-4}**	**0.04 ± 0.00**	**<0.01**	**0.77**
P5				
$\omega(NO_3^-)$	**−0.22 ± 0.07**	**88 ± 8**	**<0.01**	**0.14**
$\delta^{15}N_{NO3}$	**1.3 ± 0.5×10^{-4}**	**0.03 ± 0.01**	**0.02**	**0.08**
$\delta^{18}O_{NO3}$	**−1.6 ± 0.2×10^{-4}**	**0.08 ± 0.00**	**<0.01**	**0.56**
$\Delta^{17}O_{NO3}$	**−5.9 ± 0.6×10^{-5}**	**0.04 ± 0.00**	**<0.01**	**0.56**

Supplementary Table S2. Comparison of surface mass balances (SMB) at CHICTABA sampling sites for three time periods. SMB values are the SMB output and uncertainty of the MARv3.12.1 forced with ERA5 data from 1979–2021 (Agosta et al., 2019; Amory et al., 2021) grouped into three time subsets: the mean annual value of 2011–2013 (three years preceding sampling), the mean annual value of 1979–2021 (complete model output), and the annual value for 2013 (single year preceding sampling). Sites are ordered by distance along the traverse from the D85 starting point toward the ABN destination, and other site details can be found in Table 1.

	Surface mass balance (kg m^{-2} a^{-1})		
Site	***2011–2013***	***1979–2021***	***2013***
CHIC-01	198.8 ± 2.2	193.8 ± 2.2	174.0 ± 2.3
CHIC-02	188.7 ± 2.2	182.6 ± 2.2	164.6 ± 2.2
CHIC-03	175.0 ± 2.1	168.3 ± 2.1	151.8 ± 2.2
CHIC-04	167.2 ± 2.1	160.7 ± 2.1	144.6 ± 2.2
CHIC-05	155.8 ± 2.0	151.7 ± 2.0	133.3 ± 2.2
CHIC-06	157.5 ± 2.0	153.6 ± 2.0	135.1 ± 2.2
CHIC-07	172.3 ± 2.1	170.4 ± 2.1	151.4 ± 2.3
CHIC-08	173.7 ± 2.1	172.2 ± 2.1	153.1 ± 2.3
CHIC-09	166.9 ± 2.1	166.5 ± 2.1	147.5 ± 2.3
CHIC-10	140.2 ± 2.0	142.8 ± 2.0	123.2 ± 2.0
CHIC-11	135.3 ± 2.0	138.7 ± 2.0	119.4 ± 2.0
CHIC-12	126.4 ± 2.0	131.7 ± 2.0	112.4 ± 2.0
CHIC-13	125.9 ± 2.0	134.4 ± 2.0	114.0 ± 2.0
CHIC-14	131.2 ± 2.0	142.5 ± 2.0	121.5 ± 2.1
CHIC-15	137.2 ± 2.1	150.5 ± 2.1	129.3 ± 2.0
CHIC-16	141.3 ± 2.1	154.6 ± 2.1	136.3 ± 2.0
CHIC-17	136.4 ± 2.0	149.0 ± 2.0	133.3 ± 1.9
CHIC-18	133.6 ± 2.0	146.1 ± 2.0	130.9 ± 1.9
CHIC-19	132.6 ± 2.0	145.7 ± 2.0	130.0 ± 1.9
CHIC-20	129.8 ± 2.0	143.3 ± 2.0	126.0 ± 1.8
CHIC-21	129.0 ± 2.0	142.8 ± 2.0	125.2 ± 1.8
CHIC-22	123.9 ± 2.0	138.1 ± 2.0	121.1 ± 1.8
ABN	114.3 ± 1.9	128.0 ± 1.9	114.9 ± 1.7

Supplementary Table S3. Comparison of relationships between NO_3^- variables and surface mass balance (SMB) at CHICTABA sites for three different time subsets. Coefficients and statistics are shown for the linear regressions of NO_3^- variables versus local site SMB^{-1}, with skin layer and 1 m depth layer samples separately analyzed. Coefficient values are given with ±1 standard error. Values of SMB used in the regressions are the output of MARv3.12.1 (Agosta et al., 2019; Amory et al., 2021). Regressions were calculated using three time subsets of SMB data: the three years 2011–2013 preceding sampling, the complete output of 1979–2021, and the single year 2013 preceding sampling (Supplementary Table S2). Regressions with statistically significant ($p < 0.05$) *f-statistic* values are bolded.

Skin layer samples												
SMB years:	***2011–2013***				***1979–2021***				***2013***			
Variable	***Slope***	***Intercept***	***F-statistic p-value***	***r^2***	***Slope***	***Intercept***	***F-statistic p-value***	***r^2***	***Slope***	***Intercept***	***F–statistic p–value***	***r^2***
	(ng g^{-1} · kg m^{-2} a^{-1} or kg m^{-2} a^{-1})	*(ng g^{-1} or unitless)*			*(ng g^{-1} · kg m^{-2} a^{-1} or kg m^{-2} a^{-1})*	*(ng g^{-1} or unitless)*			*(ng g^{-1} · kg m^{-2} a^{-1} or kg m^{-2} a^{-1})*	*(ng g^{-1} or unitless)*		
$\omega(NO_3^-)$	–4227 ± 18373	290 ± 131	0.82	0.00	–6547 ± 28203	304 ± 191	0.82	0.00	–4037 ± 22663	291 ± 175	0.86	0.00
$\ln(\delta^{15}N_{NO3} + 1)$	**4.0 ± 1.5**	**0.0 ± 0.0**	**0.01**	**0.26**	**7.5 ± 2.1**	**–0.1 ± 0.0**	**<0.01**	**0.39**	**6.2 ± 1.6**	**–0.1 ± 0.0**	**<0.01**	**0.41**
$\ln(\delta^{18}O_{NO3} + 1)$	–1.4 ± 0.9	0.1 ± 0.0	0.11	0.11	–1.9 ± 1.3	0.1 ± 0.0	0.17	0.09	–1.1 ± 1.1	0.1 ± 0.0	0.33	0.04
$\ln(\Delta^{17}O_{NO3} + 1)$	0.1 ± 0.3	0.0 ± 0.0	0.71	0.01	0.4 ± 0.4	0.0 ± 0.0	0.37	0.04	0.4 ± 0.3	0.0 ± 0.0	0.22	0.07
1 m depth layer samples												
SMB years:	***2011–2013***				***1979–2021***				***2013***			
Variable	***Slope***	***Intercept***	***F-statistic p-value***	***r^2***	***Slope***	***Intercept***	***F-statistic p-value***	***r^2***	***Slope***	***Intercept***	***F–statistic p–value***	***r^2***
	(ng g^{-1} · kg m^{-2} a^{-1} or kg m^{-2} a^{-1})	*(ng g^{-1} or unitless)*			*(ng g^{-1} · kg m^{-2} a^{-1} or kg m^{-2} a^{-1})*	*(ng g^{-1} or unitless)*			*(ng g^{-1} · kg m^{-2} a^{-1} or kg m^{-2} a^{-1})*	*(ng g^{-1} or unitless)*		
$\omega(NO_3^-)$	–2626 ± 3745	91 ± 28	0.50	0.04	–3883 ± 5610	99 ± 39	0.50	0.04	–3141 ± 4892	97 ± 39	0.53	0.03
$\ln(\delta^{15}N_{NO3} + 1)$	5.1 ± 3.1	0.0 ± 0.0	0.12	0.19	8.1 ± 4.6	0.0 ± 0.0	0.10	0.21	6.9 ± 4.0	0.0 ± 0.0	0.11	0.20
$\ln(\delta^{18}O_{NO3} + 1)$	**–4.4 ± 2.0**	**0.1 ± 0.0**	**0.04**	**0.30**	**–7.5 ± 2.8**	**0.1 ± 0.0**	**0.02**	**0.38**	**–6.3 ± 2.4**	**0.1 ± 0.0**	**0.03**	**0.35**
$\ln(\Delta^{17}O_{NO3} + 1)$	–1.2 ± 0.7	0.0 ± 0.0	0.10	0.21	**–2.1 ± 0.9**	**0.0 ± 0.0**	**0.04**	**0.30**	**–1.8 ± 0.8**	**0.0 ± 0.0**	**0.05**	**0.29**

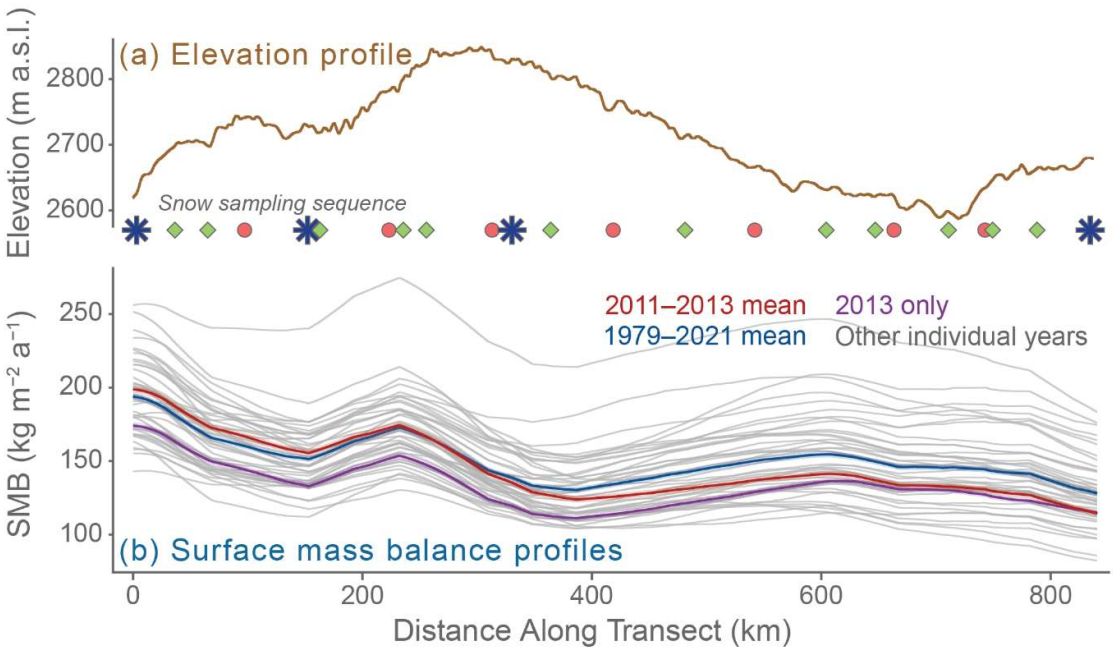

Supplementary Figure S1. Spatial changes in elevation and surface mass balance (SMB) along the CHICTABA transect. Elevation data (a) is taken from the 200 m grid REMA (Howat et al., 2019). Mean annual SMB profiles (b) for each year in 1979–2021 are shown by gray lines and are the 1 km bilinear interpolation of the 35 km MAR output grid along the CHICTABA route. Colored lines highlight the SMB profiles used in data analyses: mean of 2011–2013 (red), mean of 1979–2021 (blue), and 2013 alone (violet).

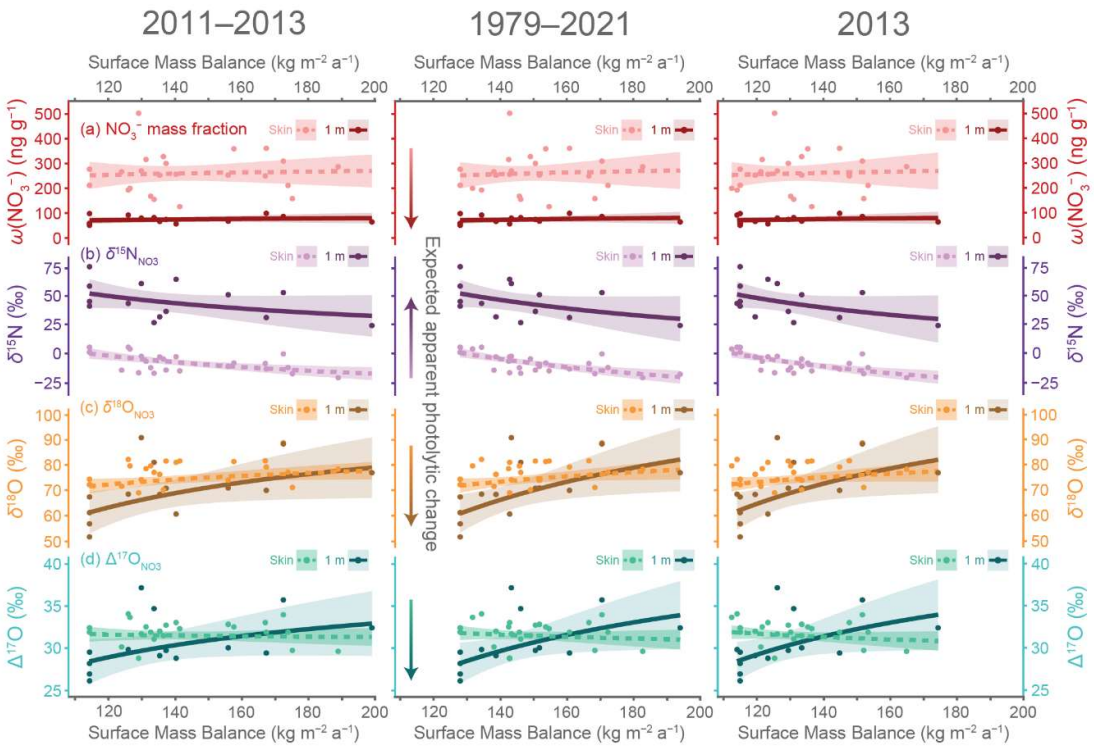

Supplementary Figure S2. Spatial relationships between nitrate variables and site surface mass balance (SMB) for three different time subsets. Linear regressions of (a) ω(NO3−) and (b–d) ln(δ_i + 1) versus SMB^{-1} are shown by dashed (skin layer) and solid (1 m depth layer) lines with 95 % confidence intervals of the regression shown by shaded zones. The SMB values are mean annual values from MARv3.12.1 (Agosta et al., 2019; Amory et al., 2021) for three time periods: 2011–2013, 1979–2021, and 2013. The SMB axes are scaled the same across all time subsets. Individual points represent individual samples. The direction of expected changes to NO_3^- variables due to photolysis is indicated by colored arrows. Regression coefficients and statistics are given in Supplementary Table S3. Note that some skin layer values in 2013 extend farther to the left than 1 m depth samples because these came from sites at around 380 km along the transect (Supplementary Figure S1) that did not have corresponding 1 m depth samples and were drier than any site with 1 m depth samples in 2013. In 2011–2013 and 1979–2021, the driest site was ABN which had both skin layer and 1 m depth samples.

References

Agosta, C., Amory, C., Kittel, C., Orsi, A., Favier, V., Gallée, H., van den Broeke, M. R., Lenaerts, J. T. M., van Wessem, J. M., van de Berg, W. J., and Fettweis, X.: Estimation of the Antarctic surface mass balance using the regional climate model MAR (1979–2015) and identification of dominant processes, The Cryosphere, 13, 281–296, https://doi.org/10.5194/tc-13-281-2019, 2019.

Amory, C., Kittel, C., Le Toumelin, L., Agosta, C., Delhasse, A., Favier, V., and Fettweis, X.: Performance of MAR (v3.11) in simulating the drifting-snow climate and surface mass balance of Adélie Land, East Antarctica, Geoscientific Model Development, 14, 3487–3510, https://doi.org/10.5194/gmd-14-3487-2021, 2021.

Favier, V., Agosta, C., Parouty, S., Durand, G., Delaygue, G., Gallée, H., Drouet, A.-S., Trouvilliez, A., and Krinner, G.: An updated and quality controlled surface mass balance dataset for Antarctica, The Cryosphere, 7, 583–597, https://doi.org/10.5194/tc-7-583-2013, 2013.

Howat, I. M., Porter, C., Smith, B. E., Noh, M.-J., and Morin, P.: The Reference Elevation Model of Antarctica, The Cryosphere, 13, 665–674, https://doi.org/10.5194/tc-13-665-2019, 2019.

Mottram, R., Hansen, N., Kittel, C., van Wessem, J. M., Agosta, C., Amory, C., Boberg, F., van de Berg, W. J., Fettweis, X., Gossart, A., van Lipzig, N. P. M., van Meijgaard, E., Orr, A., Phillips, T., Webster, S., Simonsen, S. B., and Souverijns, N.: What is the surface mass balance of Antarctica? An intercomparison of regional climate model estimates, The Cryosphere, 15, 3751–3784, https://doi.org/10.5194/tc-15-3751-2021, 2021.

Thomas, E. R., van Wessem, J. M., Roberts, J., Isaksson, E., Schlosser, E., Fudge, T. J., Vallelonga, P., Medley, B., Lenaerts, J., Bertler, N., van den Broeke, M. R., Dixon, D. A., Frezzotti, M., Stenni, B., Curran, M., and Ekaykin, A. A.: Regional Antarctic snow accumulation over the past 1000 years, Clim. Past, 13, 1491–1513, https://doi.org/10.5194/cp-13-1491-2017, 2017.

Wang, Y., Ding, M., Wessem, J. M. van, Schlosser, E., Altnau, S., Broeke, M. R. van den, Lenaerts, J. T. M., Thomas, E. R., Isaksson, E., Wang, J., and Sun, W.: A comparison of Antarctic Ice Sheet surface mass balance from atmospheric climate models and in situ observations, Journal of Climate, 29, 5317–5337, https://doi.org/10.1175/JCLI-D-15-0642.1, 2016.